

Received December 20, 2018; reviewed; accepted March 12, 2019

## Optimization and kinetics studies of lead concentrate leaching using fluoroboric acid

Arash Sobouti <sup>1</sup>, Bahram Rezai <sup>1</sup>, Fatemeh Sadat Hoseinian <sup>1</sup>, Davood Moradkhani <sup>2</sup>

<sup>1</sup> Department of Mining and Metallurgical Engineering, Amirkabir University of Technology, Tehran, Iran

<sup>2</sup> Department of Mining Engineering, University of Zanjan, Iran

Corresponding author: Arash.sobouti@aut.ac.ir (Arash Sobouti)

**Abstract:** In this study, the feasibility of lead dissolution from lead concentrate using fluoroboric acid by hydrometallurgical method was investigated in order to decrease the disadvantages of the pyrometallurgical processes. The effects of important operating parameters such as leaching time, liquid/solid ratio, stirring speed, temperature and fluoroboric acid concentration on the lead recovery were investigated using response surface methodology (RSM) based on the central composite design (CCD) model. The results show that the optimum conditions for the high lead recovery were: leaching time= 30 min, liquid/solid ratio= 10, stirring rate= 500 rpm, temperature= 80°C and fluoroboric acid concentration= 3.35 mol/L. More than 94% of lead was recovered in the optimum conditions. The results indicated that the liquid/solid ratio, fluoroboric acid concentration, temperature and leaching time were the most effective parameters on the process efficiency, respectively. Dissolution kinetics studies of lead in the fluoroboric acid were also evaluated. The chemical reaction was determined as the controlling mechanism of reaction at the shrinking core model. The activation energy was determined using Arrhenius model as 5.99 kJ/mol.

**Keywords:** lead concentrate, fluoroboric acid, hydrometallurgy, optimization, kinetics

### 1. Introduction

Lead, as an important nonferrous metal, is usually used in various fields including the electricity industry, batteries, nuclear power and radiation protection material. The lead mainly exists in nature in the form of sulphide and oxidised minerals such as galena (PbS), cerussite (PbCO<sub>3</sub>) and anglesite (PbSO<sub>4</sub>) (Feng et al., 2015).

Nowadays, the pyrometallurgical process is economically used to recover the lead from the minerals (Strunnikov and Koz'min, 2005). It has some disadvantages including high energy consumption, slag production and disposal, emission of toxic gases and air pollution (Liew, 2008). On the other hand, hydrometallurgical methods for lead extraction are more acceptable as the points of environmental aspects and low investment capital (Liew, 2008; Maccagni, 2015). The hydrometallurgical process has been efficiently used for the lead recovery in the literature. Chloride leaching of lead has received considerable attention over the last 20 years. Baba et al. (2012) compared the kinetics of galena leaching in FeCl<sub>3</sub>-HCl with H<sub>2</sub>O<sub>2</sub>-HCl systems. They obtained that the activation energy of 26.5 kJ/mol existed in the system contains 0.3 mol/L FeCl<sub>3</sub> and 8.06 mol/L HCl, while the activation energy of 40.06 kJ/mol was obtained in the presence of 8.06 mol/L of HCl and H<sub>2</sub>O<sub>2</sub>. They showed that the chemical reaction control model was the controlling mechanism for galena leaching in both systems (Baba and Adekola, 2012). Mozaffari et al (2014) studied the leaching of mercury and lead from lead concentrate of the Lake mine. They obtained 99.8% of lead by FeCl<sub>3</sub>-NaCl system (Mozaffari et al., 2014). Abdollahi et al (2015) considered the lead cementation from leaching chloride solution of lead sulfate using the aluminium powder. They indicated that the chloride leaching method was an economic and fast method (Abdollah et al., 2015). Chmielewski et al. (2017) studied the chloride leaching of silver and lead from a solid

residue after the atmospheric leaching of flotation copper concentrates. They showed that temperature was an essential parameter in the recovery of leaching. Also, the presence of oxidants was desirable for Pb and Ag leaching due to the presence of sulfides of metals in the feed (Chmielewski et al., 2017).

Chloride leaching is an effective method for lead leaching which has several advantages including low cost of leaching agents and fast dissolution of lead chloride in the chloride ion solutions with an appropriate concentration (Qin et al., 2009). But, it has some disadvantages due to specific characteristics of the chlorine ion. Therefore, some efforts have been addressed towards the definition of a process with combining the advantage of the redox pair of  $\text{Fe}^{2+}/\text{Fe}^{3+}$  as oxidant for changing the sulphide to sulphur without having the disadvantages derived using chlorine ion.

Feasible anions that can be used in substitution are:  $\text{SiF}_4^-$ ,  $\text{NH}_2^-$ ,  $\text{SO}_3^-$  and  $\text{BF}_4^-$ . In order to increase the kinetic of leaching, the process should be carried out in the temperature of 80-100°C. Fluoborate ( $\text{BF}_4^-$ ) is being perfectly stable at those temperatures and it is decomposed at the temperatures more than 130°C (Bozzano et al., 2011; Maccagni, 2014).

Wu et al. (2014) studied lead recovery from cerussite concentrate with methanesulfonic acid. They concluded that the methanesulfonic acid can be effectively used for leaching of cerussite. They extracted more than 98% lead using methanesulfonic acid (Wu et al., 2014). Wu et al. (2016) studied cerussite leaching with sulfamic acid solution. They showed that the leaching rate of cerussite increased with increasing the sulfamic acid concentration, stirring speed and temperature. Likewise, the leaching rate of cerussite increased with a decrease in the average particle size. In the optimum conditions, 95% lead was extracted. They obtained that the leaching process was controlled by the shrinking core model for surface chemical reaction (Wu et al., 2016). Amalia et al. (2017) studied the leaching behaviour of galena concentrate in fluosilicic acid solution with hydrogen peroxide. They showed that the lead extraction percentage of leaching process was 99.26% in the conditions of 97°C, 135 minutes and using -100+150 mesh of concentrate in 3.44 M of  $\text{H}_2\text{SiF}_6$  with 12% of solid percentage (Amalia et al., 2017). Ghasemi et al. (2018) studied the kinetics modelling and Alkaline leaching of lead and zinc by sodium hydroxide. They showed that the optimum conditions were NaOH concentration of 4 M, liquid/solid ratio of 20, temperature of 80°C and stirring speed of 500 rpm. Under these conditions, the highest recovery of lead was obtained to be 72.15%. The dissolution kinetics of lead was evaluated by the shrinking core models. They showed that the diffusion through the fluid film was the leaching kinetics rate controlling step of lead. The activation energy was found to be 13.6 kJ/mol (Ghasemi and Azizi, 2018).

Fluoroboric acid ( $\text{HBF}_4$ ) is an inorganic acid consisting of a strong acid with a weak coordinative conjugate base. One of the features of  $\text{HBF}_4$  as the leachant is its selectivity in dissolution process of tin and lead (IM 2003, Park and Fray, 2009). The solubility of the fluoroborate salts is higher than that of the sulfide, sulfate and chloride salts (Tan, 1992).

No study evaluated the prediction of the leaching of cerussite in fluoroborate medium in the literature. In this study, the leaching of cerussite concentrate using fluoroboric acid was comprehensively evaluated based on the optimization process and kinetic studies. In this regard, the effects of important factors such as leaching time, temperature, stirring rate, fluoroboric acid concentration and liquid/solid ratio were evaluated using the response surface methodology (RSM) based on central composite design (CCD) model. In addition, the leaching kinetics of lead concentrates was investigated using the shrinking core model.

## 2. Materials and methods

The cerussite concentrate sample was obtained from Kane Arayi Aria Company in Zanjan city, Iran. Firstly, the X-ray fluorescence (XRF) (Philips X Unique II) analysis was used to determine the composition of the samples. The results show that the sample contains the 64.8% of PbO and 10.2% of ZnO (Table 1). Then, X-ray Diffraction (XRD) (X'Pert MPD, Philips, Holland) analysis was used to determine the mineralogy of the samples. The XRD analysis (Fig. 1) showed that the sample mainly contains cerussite ( $\text{PbCO}_3$ ), mimetite ( $\text{Pb}_5(\text{AsO}_4)_3\text{Cl}$ ) and hemimorphite ( $\text{Zn}_4(\text{Si}_2\text{O}_7)_2 \cdot \text{H}_2\text{O}$ ). The Philips XL30 model scanning electron microscopy equipped with WDX (wavelength-dispersive X-ray spectroscopy) was used to compare the morphology of the solid particle sample before and after leaching.

Table 2 shows the size distribution analysis of lead concentrate. The results show that 93.6% of the feed is below 53 micron which is an appropriate size for leaching. Different fractions of the samples were also analyzed to calculate lead distribution in specified sections. According to Table 2 and Fig. 2, lead grade has the same distribution in different sizes.

Table 1. XRF of the sample (mass fraction, %)

MgO	Al <sub>2</sub> O <sub>3</sub>	SiO <sub>2</sub>	P <sub>2</sub> O <sub>5</sub>	S	Cl	K <sub>2</sub> O	CaO	TiO <sub>2</sub>
0.69	0.23	2.1	0.097	2.01	0.45	0.041	0.62	0.17
MnO	Fe <sub>2</sub> O <sub>3</sub>	CuO	Ag <sub>2</sub> O	CdO	SrO	As <sub>2</sub> O <sub>3</sub>	ZnO	PbO
0.021	2.28	0.044	0.03	0.065	0.013	4.6	10.2	64.8

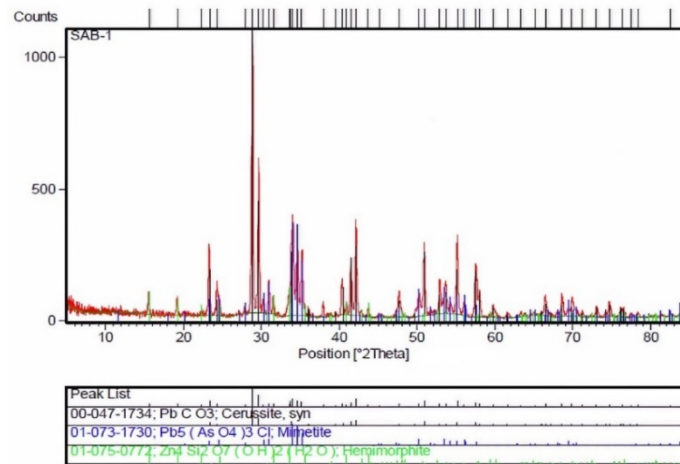


Fig. 1. XRD pattern of sample before leaching

Table 2. Size distribution analysis of lead concentrate

Particle size (micron)	Weight (%)	Cumulative retained (%)	Cumulative passing (%)	Grade Pb (%)	Distribution Pb (%)
+62	4.44	4.44	95.56	62.6	4.45
-62+53	1.94	6.38	93.62	64.87	2.01
-53+45	4.86	11.24	88.76	65.91	5.13
-45+38	10.30	21.54	78.46	64.78	10.69
-38+25	13.74	35.28	64.72	65.36	14.39
-25	64.72	100.00	0.00	61.06	63.33
Total	100.00	---	---	62.4	100

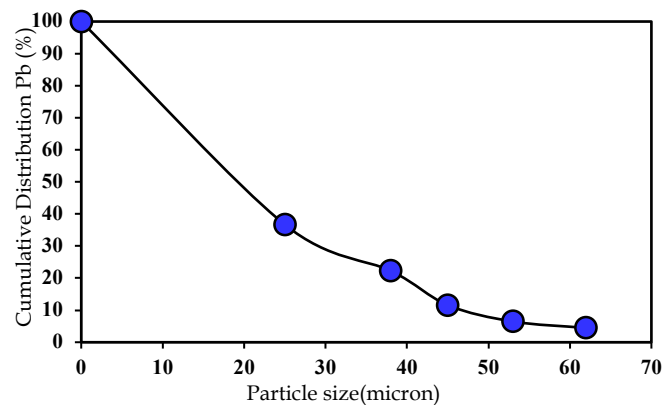


Fig. 2. Curve of distribution cumulative Pb

## 2.1. Chemical reagents and equipment

Industrial fluoroboric acid ( $\text{HBF}_4$ ) of 6.75 mol/L with analytical grade 45% (Kimia Teb Company) was used as a leaching agent. The leaching experiments were carried out in 600 ml breaker, which was heated by a hot plate, equipped with a digital controlled magnetic stirrer and a thermometer to control the temperature. A series of fluoroboric acid with various concentrations was prepared as the leaching agent and put into the beaker. A digital pH meter was used to check the pH of solution. According to the desired liquid to the solid ratio, 15 g of solid was added into the solution. Then solutions were mixed using a magnetic stirrer with a certain speed at the required temperature. When the process finished, the sample was filtered and the liquid phase was analysed with atomic adsorption spectroscopy (AAS) (Perkin Elmer AA300 model) for the Pb concentration. The experimental leaching set-up was shown in Fig 3.

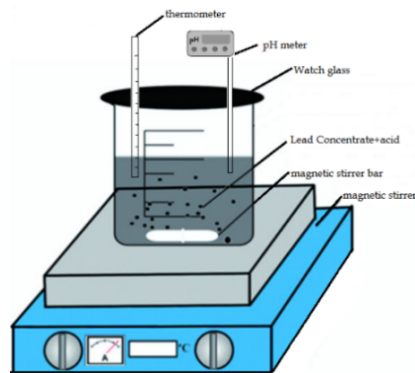


Fig. 3. Leaching experimental setup

The leaching recovery of Pb was calculated according to the equation 1 as follows (Ghasemi and Azizi, 2018):

$$R = \frac{C_M \times V}{C_0 \times M} \times 100 \quad (1)$$

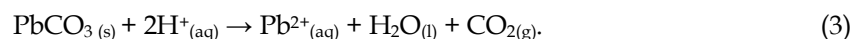
where R is the recovery percentage of Pb;  $C_M$  is the concentration of Pb ion in the leach liquor (g/L); V is the leach liquor volume (L);  $C_0$  is the concentration of Pb ion in the sample (%) and M is the mass of the Pb ore concentrate (g).

## 2.2. Leaching reactions

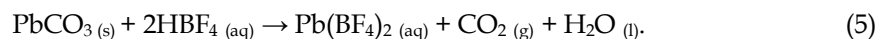
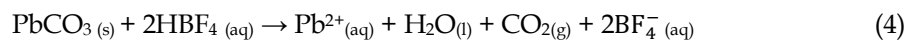
Fluoroboric acid in the aqueous medium had the following reaction:



When cerussite was added into the fluoroboric acid solution, the reaction for cerussite leaching during the process is as follows:



Consequently, the overall leaching reactions can be written as follows:



## 2.3. Mechanism and kinetic model determination

The first and second order reaction rates have been suggested for many reactions. The recovery equations for first and second order are as follows (Levenspiel 1999):

For the first order reaction:

$$kt = -\ln(1-x) \quad (6)$$

For the second order reaction:

$$kt = x/(1-x) \quad (7)$$

where x is the Pb extraction, k is the kinetic constant and t is the reaction time.

For a liquid/solid reaction system, the reaction rate is generally controlled by one of these steps: diffusion through the liquid film, diffusion through the ash/product layer and the chemical reaction at the surface of the solid particles (Levenspiel, 1999). The shrinking core model (SCM) considers that the leaching process is controlled by one of these steps. The leaching reaction of the mineral particles with a reagent (a solid–fluid reaction) is expressed as:



The rate of the process would be controlled by the slowest of these sequential steps. The recovery-time equations for models (SCM) such as controlling by diffusion through the liquid film, diffusion through solid reaction product and surface chemical reaction are shown in Table 3.

Table 3. Equations relevant shrinking core model

Controller agent	Equation
Diffusion through the liquid film	$k_l t = x$
Diffusion through solid reaction product	$1-3(1-x)^{2/3}+2(1-x) = k_d t$
Surface chemical reaction	$1-(1-x)^{1/3} = k_r t$

where  $x$  is the conversion fraction of solid particles,  $k_l$  is the apparent rate constant for diffusion through the fluid film,  $k_r$  is the apparent rate constant for the surface chemical reaction,  $k_d$  is the apparent rate constant for diffusion through the product layer and  $t$  is the reaction time. To consider the correspondence of leaching process with control mechanisms, parameters  $kt$ ,  $1-3(1-x)^{2/3}+2(1-x)$ , and  $1-(1-x)^{1/3}$  are plotted against the reaction time and the highest correlation coefficient ( $R^2$ ) value is suggested as the acceptable model for leaching behavior (Levenspiel, 1999; Wu et al., 2016).

The Arrhenius plot can be used to evaluate the activation energy if the reaction mechanism is assumed to remain unchanged over the temperature range of the experiments. Arrhenius model was used to determine the activation energy of reaction which is obtained through the slope ( $-E/R$ ) of  $\log k$  plotted versus  $1/T$  for the each value of the temperature and the following values (Habashi, 1999):

$$E/R = -2.303a \quad (8)$$

where  $E$  is the activation energy and  $R$  is the gas constant.

The kinetic studies were evaluated at various temperatures including 40, 60, and 80°C. The leaching was carried out at 10, 20, 30, 60, 120, 240 and 360 seconds and 3 mL of pulp was sampled to determine the lead concentration.

## 2.4. Design of experimental

RSM is used to design the experiments and construct models to evaluate the effects of multiple factors and investigate the optimum conditions. It can analyse the interaction between parameters with considering the separate effect of parameters (Khataee, Fathinia et al. 2010, Guan, Deng et al. 2017).

One of the most commonly used methods in RSM is central composite design (CCD). A CCD with design model of Quadratic was used to determine the optimal conditions for the significant factors. Based on the literature and initial experiments, five main factors including fluoroboric acid concentration (A), temperature (B), stirring rate (C), liquid/solid ratio (D) and leaching time (E) were chosen to evaluate their effects on the Pb recovery. The codes and variation levels of operating parameters are listed in Table 4. Through the central composite design method, 33 experiments were designed as shown in Table 5.

## 3. Results and discussion

### 3.1. ANOVA analysis

To consider the significance of data using analysis of variance (ANOVA) as a statistical tool is recommended. In fact, it is used to analyze the effect of a parameter with more than two levels (Lazic, 2006). The lead recovery for the 33 leaching experiments is presented in Table 5. Then, ANOVA was carried out for these results to determine whether the effects of process factors are statistically significant and it was used to analyze and suggest a mathematical model based on the experimental

leaching recovery data. The variance analysis results of lead extraction are shown in Table 6. The significance of the model was evaluated using the Fisher variation ratio ( $F$  value) and probability value ( $\text{Prob}>F$ ). In the Fisher method, the significance of a model is dependent on the  $F$ -value and  $p$ -value values. The upper level of  $F$ -value and the lower level of  $p$ -value ( $p\text{-value}<0.05$ ) indicate the significance of the model at the confidence interval of 95% (Lazic, 2006; Hoseinian et al., 2018).

Table 4. Independent variables and their levels in central composite rotatable design

Variables	Symbol	Codes and levels				
		-2	-1	0	+1	+2
Fluoroboric acid concentration/(mol/L)	A	2	3	4	5	6
Leaching temperature/ $^{\circ}\text{C}$	B	30	45	60	75	90
Stirring rate/( $\text{r}\cdot\text{min}^{-1}$ )	C	200	400	600	800	1000
liquid/solid ratio	D	4	6	8	10	12
Leaching time/(min)	E	5	15	25	35	45

Table 5. Experiments designed by CCD method and obtained results

Test No.	A	B	C	D	E	Pb recovery %	
						Experimental	Predicted
1	-1	+1	+1	+1	-1	88.84	89.21
2	+1	+1	-1	+1	-1	88.39	88.24
3	+1	-1	+1	-1	+1	89.03	88.92
4	+1	-1	+1	+1	-1	88.92	88.88
5	0	0	0	0	0	90.35	90.53
6	0	0	0	0	0	90.53	90.53
7	0	0	0	0	0	90.25	90.53
8	+1	+1	+1	+1	+1	91.41	91.65
9	-1	-1	+1	+1	+1	82.48	82.83
10	-1	+1	+1	-1	+1	91.24	91.54
11	+1	+1	+1	-1	-1	82.08	81.99
12	+1	+1	-1	-1	+1	91.95	91.73
13	+1	-1	-1	+1	+1	89.19	89.02
14	0	0	0	0	0	90.34	90.53
15	-1	-1	-1	-1	+1	86.77	86.66
16	-1	-1	+1	-1	-1	75.86	75.88
17	0	0	0	0	0	90.86	90.53
18	0	0	0	0	0	90.95	90.53
19	+1	-1	-1	-1	-1	73.00	72.5
20	-1	+1	-1	+1	+1	92.09	92.33
21	-1	-1	-1	+1	-1	89.02	88.98
22	-1	+1	-1	-1	-1	79.20	79.11
23	0	0	0	+2	0	89.50	89.09
24	0	0	-2	0	0	89.08	89.58
25	0	0	+2	0	0	90.68	90.15
26	0	+2	0	0	0	93.86	93.54
27	-2	0	0	0	0	90.57	90.04
28	0	-2	0	0	0	85.22	85.51
29	0	0	0	0	0	90.64	90.74
30	0	0	0	0	+2	89.00	88.72
31	0	0	0	-2	0	78.00	78.39
32	0	0	0	0	-2	76.00	76.25
33	+2	0	0	0	0	91.13	91.63

According to Table 6, The F-value of the model is 168.96 and implies that the model is significant on a confidence level of 95% ( $p$ -value $<0.05$ ). The significance of the main effect of each variable and their interaction can be statistically determined by  $p$ -value  $< 0.05$ . The effects of A, B, D, E, AB, AC, AD, BD, CD, CE, DE, A<sup>2</sup>, B<sup>2</sup>, C<sup>2</sup> and D<sup>2</sup> present the statistical significance. The factors without significance effect are C, AE, BC, BE and E<sup>2</sup>. The leaching recovery relation including the considered parameters is modeled as follows:

$$y = -63.1 + 33.2A + 0.3B + 15.36D - 0.51E - 0.03AB - 4.47 \times 10^{-3}AC - 1.52AD + 7.56 \times 10^{-5}BD - 1.86 \times 10^{-3}CD + 5.49 \times 10^{-4}CE + 0.029DE - 1.74A^2 - 1.35 \times 10^{-3}B^2 - 5.51 \times 10^{-6}C^2 - 0.51D^2 \quad (9)$$

The "adequate precision" of the model measures the signal-to-noise ratio and the value should be higher than 4. And the value of "adequate precision" of the model at 49.937 demonstrates the presence of adequate precision for the obtained model.

The reliability of the response equation was determined by the correlation coefficient ( $R^2$ ). As shown in Fig. 4, the lead recoveries calculated by equation (9) were close to the actual values and the correlation coefficient ( $R^2$ ) was 0.9965 which indicates that the obtained response equation of lead recovery is relatively reliable.

Table 6. The ANOVA analysis results of the model for lead extraction

Source	SS	DF	MS	F-value	p-value
Model	922.39	1	46.12	168.96	< 0.0001
A	171.789	1	171.789	630.01	< 0.0001
B	96.842	1	96.842	355.15	< 0.0001
C	0.496	1	0.496	1.82	0.205
D	233.438	1	233.438	856.1	< 0.0001
E	3.832	1	3.832	14.05	0.003
AB	4.72	1	4.72	17.31	0.002
AC	12.834	1	12.834	47.07	< 0.0001
AD	149.145	1	149.145	546.97	< 0.0001
AE	0.388	1	0.388	1.42	0.258
BC	0.824	1	0.824	3.02	0.11
BD	3.525	1	3.525	12.93	0.004
BE	0.788	1	0.788	2.89	0.117
CD	8.895	1	8.895	32.62	< 0.0001
CE	19.294	1	19.294	70.76	< 0.0001
DE	5.676	1	5.676	20.82	0.001
A <sup>2</sup>	81.035	1	92.629	339.7	< 0.0001
B <sup>2</sup>	1.104	1	2.778	10.19	0.009
C <sup>2</sup>	0.374	1	1.439	5.28	0.042
D <sup>2</sup>	129.217	1	128.65	471.8	< 0.0001
E <sup>2</sup>	0.018	1	0.018	0.07	0.803
Residual Error	2.999	11	0.273		
Lack of fit	2.569	6	0.428	4.97	0.05
Pure Error	0.431	5	0.086		
Cor Total	927.554	32			

### 3.2. Optimization and confirmation test

The response surface quadratic model was analyzed by design expert software and the optimal conditions of leaching by RSM optimization were as follows: acid concentration= 3.35 mol/L, temperature= 80°C, stirring rate= 500 r/min, liquid/solid ratio= 10 and leaching time= 30 min. The predicted recovery of leaching was calculated 94.39%. In order to investigate the practicability and accuracy of the optimized result, a leaching test was carried out under the optimal conditions. The actual

recovery of leaching was 94.21%. The credibility tests verified the results compared to the experimental results.

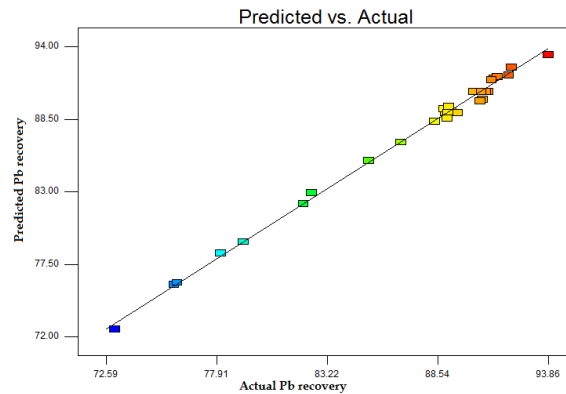


Fig. 4. Predicted Pb recovery vs actual Pb recovery

### 3.3. Effect of parameters

The perturbation plot of lead recovery (Fig. 5) shows the comparative effects of acid concentration, temperature, stirring rate, liquid/solid ratio and leaching time on the recovery of lead in the conditions of acid concentration (A)= 4.00 mol/L, temperature (B)= 60°C, stirring rate (C)= 500 r/min, liquid/solid ratio (D)= 8 and leaching time (E)= 25 min. As can be seen in Fig. 5, a sharp curvature in acid concentration, temperature and liquid/solid ratio shows that the lead recovery was very sensitive to these variables. Increasing liquid/solid ratio has increased the lead recovery and this increasing can be justified such that increasing the liquid/solid ratio increases the leaching agent and hence increasing the leaching rate (Qin et al., 2009). Increasing the lead recovery can be attributed to the fact that an increase in the L/S ratio not only decreases the suspension density, but also reduces the viscosity of the whole system and therefore decreases the mass transfer resistance at the liquid–solid interface (Abkhoshk et al., 2014).

The results show that the lead recovery is increased by increasing the acid concentration until 4.5 M of fluoroboric acid concentration and further increase in the acid concentration caused decreasing the lead recovery. When the acid concentration exceeded to a definite value, the number of hydrogen ions in the medium might decrease due to a decrease in the water amount. Additionally, this behavior can be explained by the fact that, as the acid concentration in the medium increases, the appearance rate of the product increases and as the product reaches the saturation value near the solid particle, it forms a sparingly soluble product film layer around the particle. Consequently, the dissolution process was slowed down after acid concentration of 4.5 mol/L (Imamutdinova, 1967). The lead recovery is increased with increasing the temperature because of the active molecular motion and also the reaction is endothermic (Feng et al., 2015). It was determined that increasing the temperature had a positive effect on the lead recovery. The leaching time and stirring rate curves show less sensitivity of lead recovery to changes in these variables. The stirring rate compared with acid concentration, temperature and liquid/solid ratio has no major function in the lead recovery and from the kinetic perspective, this observation indicates that the solid and liquid phases could be homogeneously mixed in the reactors, and the reaction may be controlled not by diffusion but by chemical reaction (Deng et al., 2015).

### 3.4. Interaction of parameters

The three-dimensional (3D) surfaces plots of the response surface quadratic model are shown in Fig. 5. The 3D surface plot shows the interactive influence among the various variables directly. In these plots, two variables change in the experimental ranges while the other variables are constant.

Fig. 5a shows the mutual effect of acid concentration and temperature on the lead recovery. According to literature, it is reported (Wu et al., 2014; Wu et al., 2016) that the leaching rate of cerussite in other leaching agent solutions such as MSA, sulfamic acid is increased by increasing the temperature.

As can be seen, increasing the temperature enhances the recovery at all acid concentrations although the slope is higher at lower acid concentrations.

According to literature, it is reported (Deng et al., 2015; Kocan and Hicsonmez, 2018) that increasing temperature supplies enough energy for atomic and molecular collisions and the interaction between particles of sample and fluoroboric acid increases the dissolution rate. In addition, mass transfer coefficient, reaction constant and diffusivity are promoted by increasing temperature.

Fig. 5b shows the mutual effect of acid concentration and L/S ratio on the lead recovery. According to Fig. 4, lead recovery is decreased simultaneously with increasing acid concentration and L/S ratio. Increasing the liquid/solid ratio increases the leaching agent and increasing the acid concentration causes to decrease the lead recovery. When the acid concentration enhanced from a definite value, the number of hydrogen ions in the medium might decrease more and more due to the decrease in the water amount.

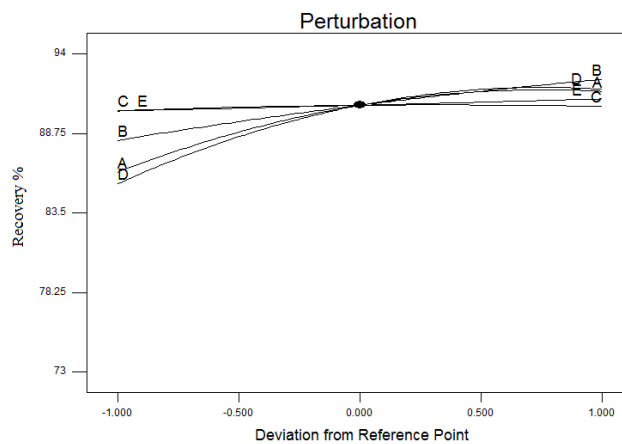


Fig. 4. Perturbation plot for recovery of lead

Fig. 5c shows the mutual effect of L/S ratio and temperature on the lead recovery. As can be seen, at higher L/S ratios, the recovery is increased with increasing the leaching agent. In the lower amount of L/S ratios, the temperature has a weaker effect on the lead recovery. The temperature has a significant positive effect on the lead recovery. According to literature, it is reported (Song et al., 2016) that with increasing the leaching temperature, the extension of lixiviant molecules in leaching solution speeds up, more easily attacks the mineral grains and the stockpile energy of mineral particles increases, so the ability of damage or weakening of the chemical bonds of mineral enhances, and the number of molecules whose kinetic energy is equal to or greater than activation energy increases.

Fig. 5d shows the mutual effect of interaction between L/S ratio and leaching time on the lead recovery. As can be seen, at higher L/S ratios, the recovery is increased with increasing the leaching agent. Generally, the leaching recovery increases with reducing the pulp density due to the high amount of leaching agent is added to a low content of solid (Habashi, 1999). No significant change was observed at lower L/S ratios due to the fact that leaching agent was reduced.

### 3.5. Scanning Electron Microscopy

Fig. 6 shows the SEM results of the samples before leaching. Micromorphological study of the sample before leaching showed that Cerussite (Ce), Mimetite (Mi), Galena (G), Hemimorphite (Hm), Sphalerite, pyrite (Py) are present in the sample. According to Fig. 6b and 6g, in large quantities of the sample in the presence of Pb and without S, there is cerussite. In the Light particles with the simultaneous presence of Pb and Cl and as is Mimetite (Mi) (Fig. 6b and 6c and 6h). In the WDX elemental map, the simultaneous presence of Pb and S is Galena (G). The presence of Zn and Si without S is Hemimorphite (Hm). The simultaneous presence of Zn and S is Sphalerite. The simultaneous presence of Fe and S is pyrite (Py). According to Fig. 6c, it seems that some As elements are replaced in the structure of Cerussite.

### 3.6. Characterization of the leach residue

The XRD pattern of the residue obtained after leaching at the optimum conditions is shown in Fig. 7. The major phases of the leach residue are lead sulfate ( $\text{PbSO}_4$ ), lead sulphide ( $\text{PbS}$ ) and Zinc sulphide ( $\text{ZnS}$ ). In addition, SEM with WDX analysis confirmed the indications reached by XRD analysis (Fig. 8). According to SEM analysis, the residue contains Anglesite ( $\text{PbSO}_4$ ), Galena ( $\text{PbS}$ ), Sphalerite ( $\text{ZnS}$ ), pyrite ( $\text{FeS}_2$ ) and As element in the structure of Anglesite, Galena.

The  $\text{PbSO}_4$  was generated from soluble Pb that reacted with  $\text{SO}_4^{2-}$  which was produced from the oxidation of  $\text{PbS}$  (Amalia et al., 2017). Galena, Sphalerite, pyrite and As element were identified in the residue indicating that these minerals had been undissolved.

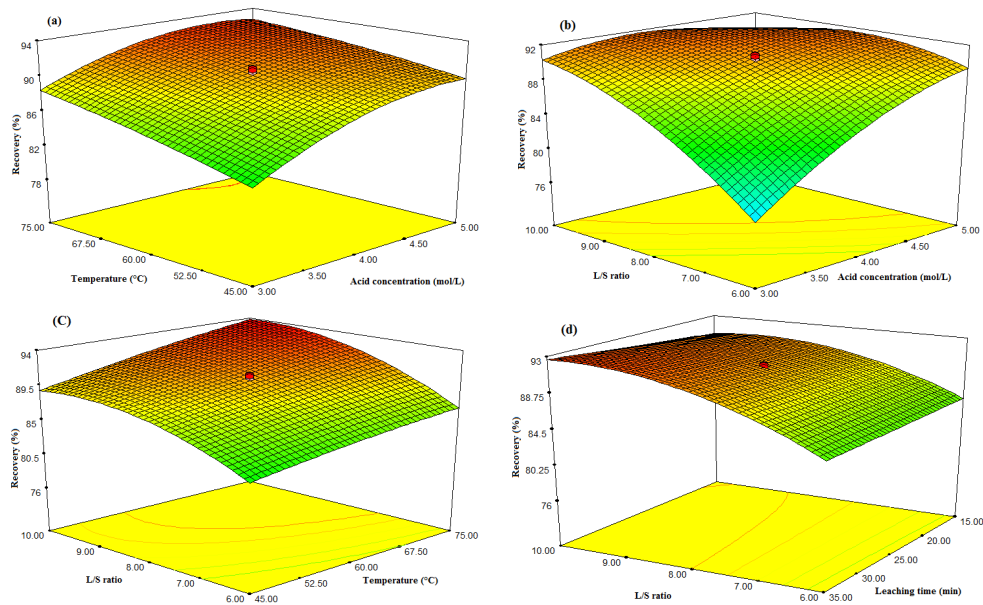


Fig. 5. Effect of leaching parameters on Pb recovery

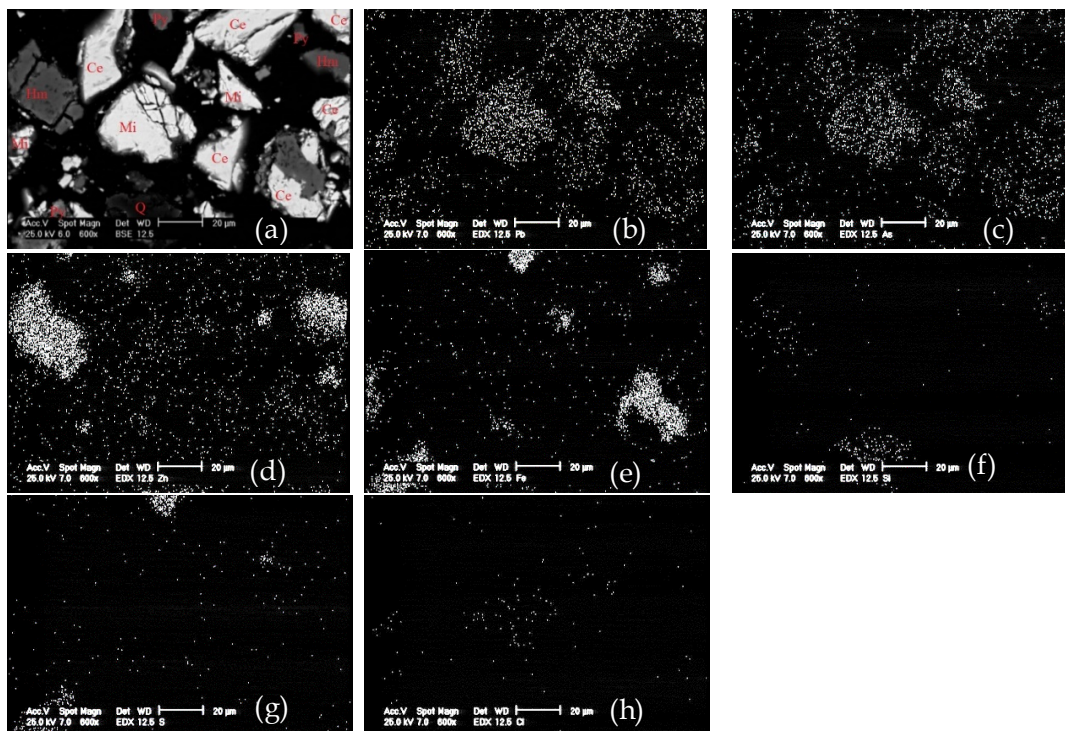


Fig. 6. SEM images of (a) samples before leaching, (b) Pb distribution map, (c) As distribution map, (d) Zn distribution map, (e) Fe distribution map, (f) Si distribution map, (g) S Distribution map, (h) Cl distribution map

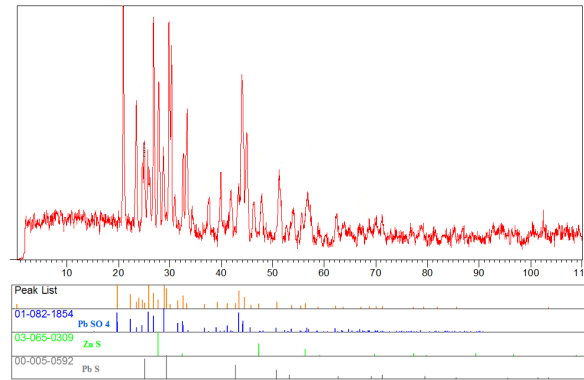


Fig. 7. XRD pattern of sample after leaching

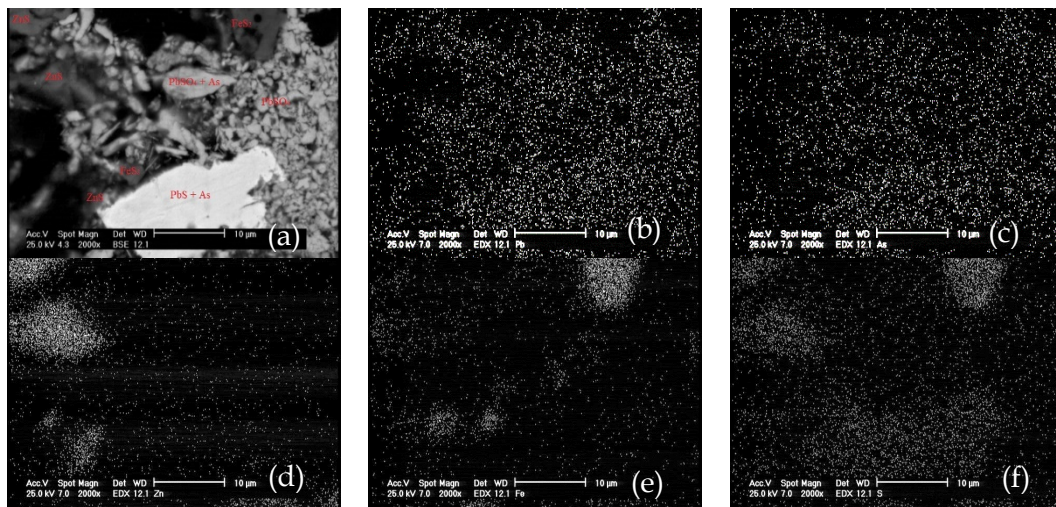
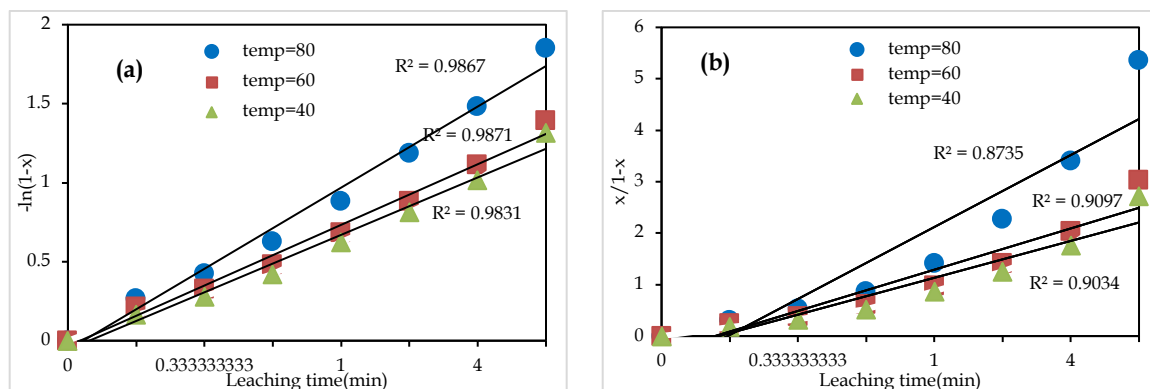


Fig. 8. SEM images of (a) residue after leaching, (b) Pb distribution map, (c) As distribution map, (d) Zn distribution map, (e) Fe distribution map, (f) S distribution map

### 3.7. Kinetic Analysis

In this work, the SCM was employed to describe the leaching rate of cerussite concentrates. In order to discover the mechanism has been changed during leaching, the equation corresponding to one of the mechanisms should be considered for the whole period of leaching.

The kinetic study was carried out to obtain an appropriate kinetic model for the lead dissolution under the optimized condition obtained based on the software outputs. According to equations (6) and (7),  $-\ln(1-x)$  and  $x/(1-x)$  against time were plotted at different temperatures as shown in Fig. 9.

Fig. 9. Diagram show the (a)  $-\ln(1-x)$  versus time, (b)  $x/(1-x)$  versus time

Comparing the correlation coefficients of these diagrams shows that the coefficient is relatively one in the first order reaction. To determine the mechanism of leaching and the rate-controlling step of cerussite concentrate dissolution in  $\text{HBF}_4$ , the experimental data were obtained in the leaching step and analyzed based on the SCM using the rate expression given in equation in Table 3 and shown in Figs. 10a, 10b and 10c, respectively. The best value of correlation coefficient was obtained through the surface chemical reaction model indicating that the model acts as the rate-controlling step in the leaching system.

The activation energy may be calculated using the Arrhenius equation (Eq. 8) and the Arrhenius plot of the dissolution process was shown in Fig. 10d. According to Fig. 10d, an activation energy of 5.99 kJ/mol can be estimated for the leaching.

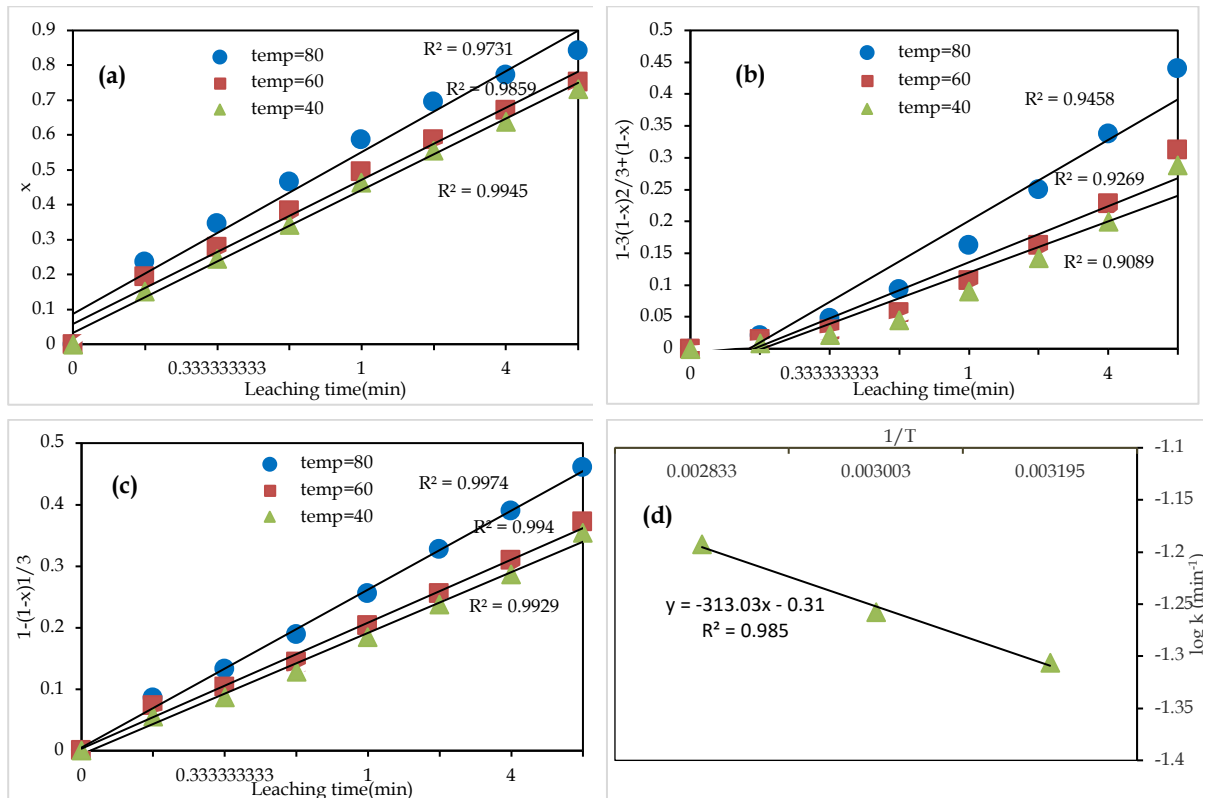


Fig. 10. Diagram shows the (a)  $x$  versus time, (b)  $1-3(1-x)^2/3+2(1-x)$  versus time, (c)  $1-(1-x)^{1/3}$  versus time, (d) Arrhenius plot

#### 4. Conclusions

This work studied the effect of operating parameters on the lead recovery using the fluoroboric acid. The results showed that the most significant parameters in the leaching tests were: Liquid/solid ratio, fluoroboric acid concentration, temperature and leaching time, respectively. The proposed model equation using RSM has shown good agreement with the experimental data with a correlation coefficient ( $R^2$ ) of 0.9965. The results of analysis of variance (ANOVA) demonstrated that the prediction of the model for lead recovery is significant. The predicted optimum conditions for maximum lead recovery by software were: leaching time= 30 min, liquid/solid ratio= 10, stirring rate= 500 rpm, temperature=80°C, and fluoroboric acid concentration= 3.35 mol/L. In the optimum conditions, 94.21% of lead was recovered. Based on ANOVA and experimental model, the liquid/solid ratio, fluoroboric acid concentration, temperature and leaching time were suggested as the most effective parameters on the lead recovery, respectively. The kinetics of leaching process was similar to the first-order reaction rate and the kinetic rate was determined 0.2566  $\text{min}^{-1}$  at 80°C. Additionally, the chemical reaction was determined as the controlling mechanism of reaction at the shrinking core model. The Arrhenius diagram was plotted for leaching reaction and activation energy of 5.99 kJ/mol was obtained.

## Acknowledgments

This research project is supported by Kane Arayi Aria Company. Hereby the authors wish to acknowledge for their financial support.

## References

- ABDOLLAHI, P., YOOZBASHIZADEH, H., MORADKHANI, D., BEHNIAN, D. (2015). *A study on cementation process of lead from brine leaching solution by aluminum powder*. Library Journal 2, 1-6.
- ABKHOSHK, E., JORJANI, E., AL-HARAHSEH, M., RASHCHI, F., NAAZERI M., 2014. *Review of the hydrometallurgical processing of non-sulfide zinc ores*. Hydrometallurgy 149, 153-167.
- AMALIA, D., Y. Ramanda and M. Maryono 2017. *Extraction of lead from galena concentrates using fluosilic acid and peroxide*. Indonesian Mining Journal 20(1), 69-80.
- BABA, A.A., ADEKOLA, F.A., 2012. *A study of dissolution kinetics of a Nigerian galena ore in hydrochloric acid*. Journal of Saudi Chemical Society 16(4), 377-386.
- BOZZANO, G., DENTE, M., PIERUCCI, S. MACCAGNI, M. 2011. *Modeling and Simulation of the Production of Lead and Elementary Sulphur from Lead Sulphide Concentrates*. Computer Aided Chemical Engineering, Elsevier. 29, 1733-1737.
- CHMIELEWSKI, T., GIBAS, K., BOROWSKI, K., ADAMSKI, Z., WOZNIAK, B., MUSZER, A., 2017. *Chloride leaching of silver and lead from a solid residue after atmospheric leaching of flotation copper concentrates*. Physicochem. Probl. Miner. Process 53(2), 893-907.
- DENG, J., SUN, Q., LIN, P., SONG, G., WEN, S., DENG, J., WU, D., 2015. *Dissolution kinetics of zinc oxide ore with an organic acid*. International Journal of Metallurgical & Materials Engineering 1, 109.
- FENG, Q.-C., WEN, S.-M., WANG, Y.-J., CAO, Q.-B., ZHAO, W.-J., 2015. *Dissolution kinetics of cerussite in an alternative leaching reagent for lead*. Chemical Papers 69(3), 440-447.
- FENG, Q., WEN, S., WANG, Y., ZHAO, W., DENG, J., 2015. *Investigation of leaching kinetics of cerussite in sodium hydroxide solutions*. Physicochemical Problems of Mineral Processing 51.
- GHASEMI, S.M.S., AZIZI, A., 2018. *Alkaline leaching of lead and zinc by sodium hydroxide: kinetics modeling*. Journal of Materials Research and Technology 7(2), 118-125.
- GUAN, S., DENG, F., HUANG, S.-Q., LIU, S.-Y., AI, L.-X, SHE, P.-Y., 2017. *Optimization of magnetic field-assisted ultrasonication for the disintegration of waste activated sludge using Box-Behnken design with response surface methodology*. Ultrasonics sonochemistry 38: 9-18.
- HABASHI, F., 1999. *Kinetics of metallurgical processes*, Métallurgie Extractive Québec.
- HABASHI, F., 1999. *A textbook of hydrometallurgy*, Métallurgie Extractive.
- HOSEINIAN, F., REZAI, B., KOWSARI, E., 2018. *Optimization and separation mechanism of Ni (II) removal from synthetic wastewater using response surface method*. International Journal of Environmental Science and Technology, 1-10.
- IM, D. (2003). *Recovery of solder and electronic components from printed circuit boards*. Electrochemistry in Mineral and Metal Processing VI: Proceedings of the International Symposium, The Electrochemical Society.
- IMAMUTDINOVA, V., 1967. *Kinetics of dissolution of borates in mineral acid solutions*. Zh. Prikl. Khim. 40, 2593-2596.
- KHATAEE, A., FATHINIA, M., ABER, S., ZAREI, M., (2010). *Optimization of photocatalytic treatment of dye solution on supported TiO<sub>2</sub> nanoparticles by central composite design: intermediates identification*. Journal of hazardous materials 181(1-3), 886-897.
- KOCAN, F. HICSONMEZ, U., 2018. *Leaching of celestite in sodium hydroxide solutions and kinetic modelling*. Journal of Dispersion Science and Technology, 1-12.
- LAZIC, Z.R., 2006. *Design of experiments in chemical engineering: a practical guide*, John Wiley & Sons.
- LEVENSPIEL, O., 1999. *Chemical reaction engineering*. Industrial & engineering chemistry research 38(11), 4140-4143.
- LIEW, F., 2008. *Pyrometallurgy versus hydrometallurgy*. TES-AMM Singapore.(www. tes-amm. com. au/downloads/ TES-AMM\_analysis\_pyrometallurgy\_vs\_hydrometallurgy\_ April\_2008. pdf).
- MACCAGNI, M., 2014. *New Approaches on Non Ferrous Metals Electrolisis*. Chemical Engineering Transactions 41, 61-66.
- MACCAGNI, M., NIELSEN, J., HYMER, T., 2015. *The FLUBOR® Process: Pilot Tests Results*. Proceedings of European Metallurgical Conference 2015 & Lead-Zinc 2015.

- MOZAFFARI, E., MOHSENI, M., ABAIE, E. 2014. *Recovering Lead Metal from Lak Mine Lead Concentrate by Ferric Chloride Leaching*. Pure and Applied Science & Technology 4(2), 37-43.
- PARK, Y. J., FRAY, D. J. 2009. *Recovery of high purity precious metals from printed circuit boards*. Journal of Hazardous Materials 164(2-3), 1152-1158.
- QIN, W.-Q., HUI, L., TANG, S.-H., WEI, S., 2009. *Preparation of lead sulfate powder directly from galena concentrates*. Transactions of Nonferrous Metals Society of China 19(2), 479-483.
- SONG, K., YUAN, J., SHEN, P., YAN, S., LI, F. LIU, D., 2016. *Leaching performance of low grade zinc oxide ore in the system of NH<sub>3</sub>-(NH<sub>4</sub>)<sub>2</sub>SO<sub>4</sub>-H<sub>2</sub>O*. 2015 4th International Conference on Sustainable Energy and Environmental Engineering, Atlantis Press.
- STRUNNIKOV, S. KOZ'MIN, Y.A., 2005. *Hydrometallurgical schemes of lead concentrate processing*. Chemistry for Sustainable Development 13(4), 483-490.
- TAN, A., 1992. *Tin and Solder plating in the semiconductor industry*, Springer Science & Business Media.
- WU, D., CUI, C., WEN, S., DENG, J., 2016. *Kinetics of Cerussite Leaching in Sulfamic Acid Solution*. Journal of Chemical Engineering of Japan 49(5), 445-451.
- WU, Z., DREISINGER, D.B., URCH, H., FASSBENDER, S., 2014. *Fundamental study of lead recovery from cerussite concentrate with methanesulfonic acid (MSA)*. Hydrometallurgy 142, 23-35.